

See discussions, stats, and author profiles for this publication at: <https://www.researchgate.net/publication/372249152>

How Flies See Motion

Article in Annual Review of Neuroscience · July 2023

DOI: 10.1146/annurev-neuro-080422-111929

CITATIONS

6

READS

52

2 authors, including:



Lukas Groschner

25 PUBLICATIONS 1,185 CITATIONS

SEE PROFILE

How Flies See Motion

Alexander Borst and Lukas N. Groschner

Max Planck Institute for Biological Intelligence, Martinsried, Germany;
email: alexander.borst@bi.mpg.de, lukas.groschner@bi.mpg.de

Annu. Rev. Neurosci. 2023.46:17–37

The *Annual Review of Neuroscience* is online at
neuro.annualreviews.org<https://doi.org/10.1146/annurev-neuro-080422-111929>

Copyright © 2023 by the author(s). This work is licensed under a Creative Commons Attribution 4.0 International License, which permits unrestricted use, distribution, and reproduction in any medium, provided the original author and source are credited. See credit lines of images or other third-party material in this article for license information.

ANNUAL REVIEWS CONNECT

www.annualreviews.org

- Download figures
- Navigate cited references
- Keyword search
- Explore related articles
- Share via email or social media

Keywords

visual system, motion detection, direction selectivity, neural computation, multiplicative disinhibition, *Drosophila*

Abstract

How neurons detect the direction of motion is a prime example of neural computation: Motion vision is found in the visual systems of virtually all sighted animals, it is important for survival, and it requires interesting computations with well-defined linear and nonlinear processing steps—yet the whole process is of moderate complexity. The genetic methods available in the fruit fly *Drosophila* and the charting of a connectome of its visual system have led to rapid progress and unprecedented detail in our understanding of how neurons compute the direction of motion in this organism. The picture that emerged incorporates not only the identity, morphology, and synaptic connectivity of each neuron involved but also its neurotransmitters, its receptors, and their subcellular localization. Together with the neurons' membrane potential responses to visual stimulation, this information provides the basis for a biophysically realistic model of the circuit that computes the direction of visual motion.

Contents

MODELS OF MOTION DETECTION	18
THE FLY VISUAL SYSTEM AND ITS TWO MOTION PATHWAYS	21
ON and OFF Pathways	23
T4 AND T5 CELLS	23
General Properties	23
Input Organization	25
Biophysical Mechanisms of Direction Selectivity	27
Multiplicative Disinhibition	29
MOTION OPPONENTY BY LOBULA PLATE INTRINSIC CELLS	30
REMAINING QUESTIONS	32

MODELS OF MOTION DETECTION

As expressed so aptly by Exner (1894), motion vision is a perception *sui generis*, a sense of its own. Indeed, when sitting in an IMAX movie theater confronted with wide-field panoramic flow fields, the illusion of self-motion is inescapable, even though the vestibular system delivers zero signal. Wide-field motion is an essential component of the perception of self-motion and necessary for visual navigation and course control in humans and animals alike. Motion stimuli play an equally important role when restricted to a small section of visual space, for example, when a predator (or a car, as its modern-day equivalent) is approaching or a prey is trying to escape from a hunter (Ache et al. 2019; for a review, see Peek & Card 2016). In both cases, detecting the direction of the moving object can be critical for the fate of the observer. Not only the survival of the individual in the short term but also the long-term survival of its lineage often depend on motion vision, since animals use local motion cues to find potential mates (Hindmarsh Sten et al. 2021, Ribeiro et al. 2018). But how does the nervous system extract this important information from the visual scene? A single photoreceptor cannot tell whether something is moving from the left to the right or the other way around. To detect the direction in which something moves, the signals derived from at least two adjacent image points have to be compared over time (Borst & Egelhaaf 1989) (**Figure 1a**). Since motion along one direction elicits sequential signals at neighboring locations, most models of motion detection propose to delay the signal derived from image point A and measure its coincidence with the signal from adjacent point B. Depending on the speed, the temporal overlap will be high for motion from point A to B, the preferred direction, and low for motion from point B to A, the nonpreferred or null direction. However, a simple summation of the signals does not measure coincidence since the temporal integrals of the responses are identical for the two directions. What is needed is a nonlinear combination of the two signals. For example, a summation followed by a threshold ($S_A + S_B$) or a multiplication ($S_A \times S_B$) (**Figure 1a**).

The first model that described this idea and proposed a way of how this could be achieved by the nervous system was published, again, by Exner (1894) (**Figure 1b**). He envisaged that signals derived from neighboring image points would spread symmetrically into opposite directions. Given a constant travel speed of the neural signal, the summation of signals on opposite sides would then lead to different results, depending on the sequence of events on the retina (Exner 1894). Half a century later, Hassenstein & Reichardt (Hassenstein & Reichardt 1956, Reichardt 1961), inspired by their behavioral observations of a tethered beetle walking on a spherical treadmill, proposed their famous correlation-type motion detector, commonly referred to as the Hassenstein–Reichardt detector in the recent literature (**Figure 1c**). Like Exner, they based

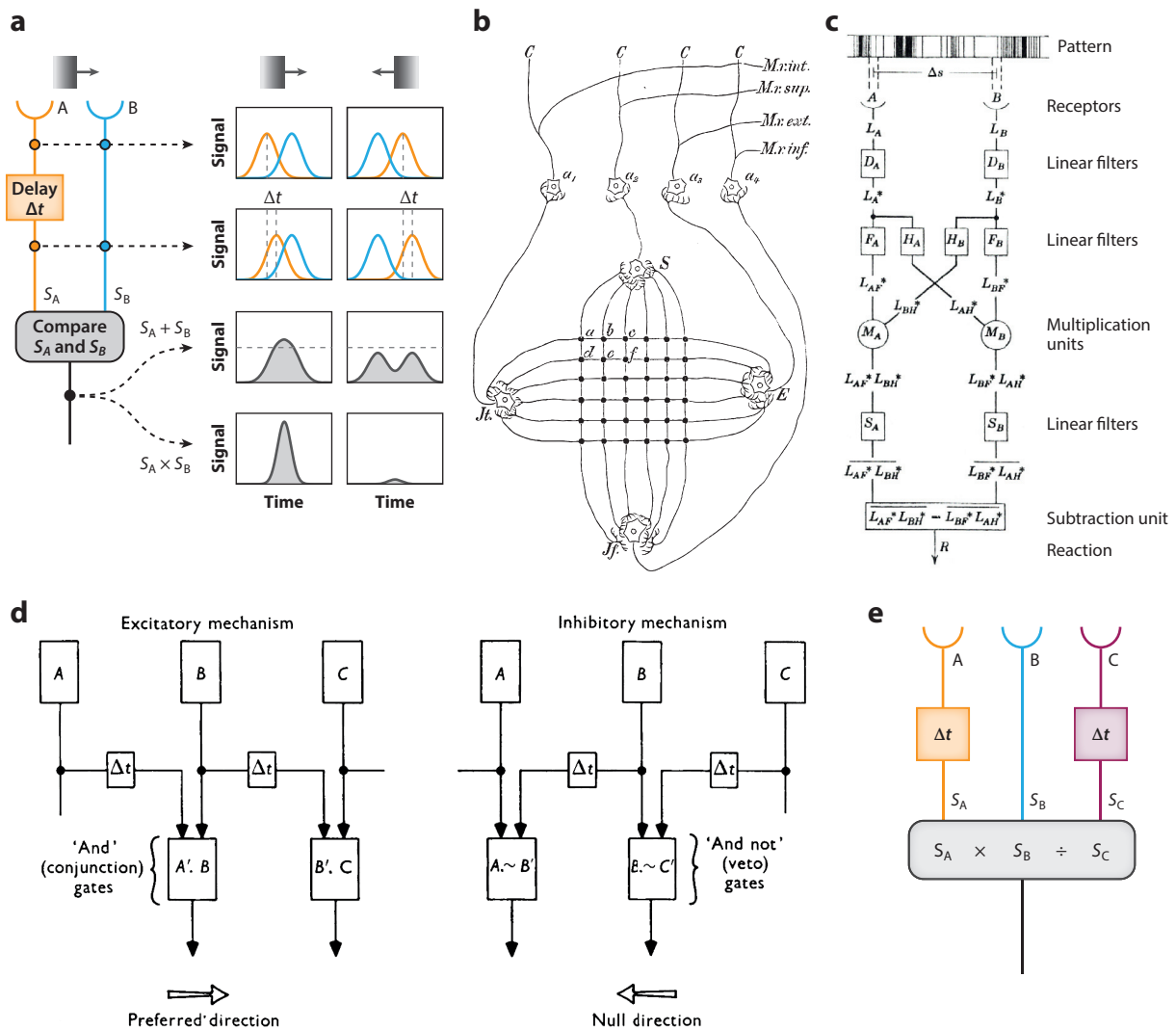


Figure 1

Models of motion detection. (a) A visual motion detector requires at least two input signals (S_A and S_B) from adjacent photoreceptors (A and B). The signals are differentially delayed by Δt so that they coincide at the detector only if A is activated prior to B, as is the case for motion in the preferred direction (rightward) but not for motion in the opposite direction. A nonlinear interaction is required to detect the coincidence of S_A and S_B . The bottom two rows of graphs show a signal summation ($S_A + S_B$) followed by a threshold (horizontal dashed line) and a signal multiplication ($S_A \times S_B$). (b) Early proposal of a motion detection circuit. Panel b reproduced from Exner (1894) (public domain). (c) Correlation or Hassenstein-Reichardt detector. Photoreceptor signals from adjacent image points are differentially filtered in time (F and H) and multiplied (M) in a mirror-symmetrical way. The outputs of the multipliers are subtracted. Panel c reproduced with permission from Reichardt (1961); copyright 1961, Massachusetts Institute of Technology. All rights reserved. (d) Preferred direction excitation and null direction inhibition, realized by AND (left) and AND NOT (right) gates, respectively, as two alternate mechanisms underlying direction selectivity in the rabbit retina. Panel d reproduced with permission from Barlow & Levick (1965). (e) A combination of the two mechanisms within one stage, as proposed by Haag et al. (2016, 2017) and Leong et al. (2016).

their model on a coincidence detection of signals derived from neighboring image points after one of them has been delayed with respect to the other. In the Hassenstein–Reichardt detector, the delay is explicitly created by linear filters, and the coincidence is registered by a multiplication. The whole process takes place twice in mirror-symmetrical subunits, the output signals of which are subtracted to form the final local motion detector signal. The mathematical formulation of this model involves precisely specified operations like multiplication, subtraction, and linear filters whose time-constants define the signal amplitude and phase delay or advance as a function of input frequency. Unlike Exner’s proposal, the Hassenstein–Reichardt detector makes no reference to the nervous system; it describes all operations in a purely algorithmic form. Another important point is that the output of the detector is fully motion-opponent, meaning that motion in opposite directions elicits signals that are identical in shape but opposite in sign, that is, positive for motion along the preferred direction and negative for motion in the null direction. A variant of the Hassenstein–Reichardt model was proposed by Barlow & Levick (1965) (**Figure 1d**). Instead of a multiplication, however, they proposed a gating mechanism by which one signal allows another one to pass or not. Barlow & Levick thought about two possible implementations: In one case, very much like the multiplier in the Hassenstein–Reichardt detector, the delayed signal derived from location A is gating a signal from location B such that motion from A to B is facilitated. They called this mechanism preferred direction excitation. Alternatively, they proposed a mechanism where signal transmission is blocked for motion from B to A. In this case, the delay sits in the other arm and provides input to an AND NOT (veto) gate, which can be approximated, arithmetically, by a division. Barlow & Levick called this mechanism null direction inhibition. Both mechanisms are combined by the three-arm detector model (**Figure 1e**), proposed by Haag et al. (2016) and Leong et al. (2016) based on their recordings from fly motion-sensitive neurons. Here, experimental results could be best described by multiplying the delayed signal (S_A) on the preferred side, that is, where a preferred motion stimulus enters the receptive field of the neuron, with the non-delayed signal derived from the center (S_B), and dividing it by the delayed signal (S_C) from the null side, that is, where a stimulus moving in the null direction enters the receptive field.

As mentioned above, all these models measure the degree of temporal overlap between the signals from neighboring image locations. As a consequence, their output, while being sensitive to the direction of image motion, depends on the speed at which the projection of an object is traveling on the retina. Obviously, given a fixed delay, there is an optimal speed at which the overlap is maximal. Motion at any speed that falls short of, or exceeds, this optimum yields an output signal of lower amplitude. Therefore, such detectors do not act like speedometers with a linear dependency on image speed but rather with a function that follows an inverted U shape. Furthermore, the output signal changes as a function of image contrast, depending on the exact type of nonlinearity involved. These and many other, often nonintuitive, predictions derived from the Hassenstein–Reichardt detector were tested in the fly visual system at the behavioral level (Borst & Bahde 1986, Buchner 1976, Götz 1964) and by recordings from large course-control neurons (lobula plate tangential cells; see below). The animals’ responses to stimuli of varying frequencies and contrasts and even to optical illusions (Clark et al. 2011, Leonhardt et al. 2017, Tuthill et al. 2011) are in exquisite quantitative agreement with model predictions (for a review, see Borst 2014). This finding has led to the strong belief that the overall structure and operations, as defined algorithmically by the Hassenstein–Reichardt detector (delay, multiplication, subtraction), must have their neuronal counterparts in the fly visual system. Further below, we discuss which neuronal elements correspond to what processing stages in the detector model and what biophysical mechanisms underlie these operations.

THE FLY VISUAL SYSTEM AND ITS TWO MOTION PATHWAYS

Fruit flies are known to have large compound eyes, built from approximately 750 facets, or ommatidia, on each side of the head capsule (**Figure 2a**). Each ommatidium contains eight different photoreceptors (R1–R8) sitting underneath a tiny lens with a diameter of only 16 μm and a focal length of 20 μm (Stavenga 2003a,b). Photoreceptors house their photopigments in membrane-rich structures called microvilli, the tips of which are located exactly within the focal plane of the lens. These tiny dimensions put practically all objects beyond a distance of a few millimeters at infinity focus, making accommodation superfluous. Within the ommatidium, the outer photoreceptors R1–R6 sit in a ring around the inner two photoreceptors R7 and R8, which are stacked on top of each other. Outer photoreceptors all have a common green-sensitive rhodopsin as a photopigment (Harris et al. 1976, O'Tousa et al. 1985) and form the major input to the motion vision system (Heisenberg & Buchner 1977, Yamaguchi et al. 2008). Inner photoreceptors R7 and R8 have photopigments with different spectral sensitivities, depending on whether they sit in a pale or in a yellow ommatidium and subserve color vision, which contributes little to motion processing (Longden et al. 2021, Wardill et al. 2012). The two classes of ommatidia tile the retina in a mosaic whose pattern is defined by the stochastic expression of the spineless transcription factor (Wernet et al. 2006). All photoreceptors have a receptive field of about 5° in diameter at half-maximum sensitivity. The optical axes of neighboring ommatidia are separated by an interommatidial angle of approximately 5° as well, resulting in a deplorable spatial resolution (Götz 1964). Together, however, they cover almost the entire visual space, allowing for panoramic vision without the need to move the head or the eyes. Active movements of the retinae might, nonetheless, improve depth perception through motion parallax, prevent unwanted receptor adaptation, and increase visual acuity (Fenk et al. 2022).

The fly devotes at least half of its brain—the optic lobes underneath its eyes (Raji & Potter 2021)—exclusively to image processing (**Figure 2a**). The different sections of the optic lobe are called the lamina, medulla, lobula, and lobula plate. Each neuropil repeats the columnar structure of the facet eye, giving rise to a highly ordered, almost crystalline, retinotopic structure (**Figure 2b**). The retinotopy is evident from the anatomy (**Figure 2a**) as well as from recent functional experiments, in which tilting the imaging plane of a two-photon microscope provided a direct glimpse of the retinotopic activity map (Schuetzenberger & Borst 2020). Throughout the four neuropils, approximately 100 different cell types can be found within each column (**Figure 2c**). This roughly corresponds in complexity to an estimate of the anatomically defined cell types in the mouse retina (Masland 2012). Initially, the catalog of cell types was drawn from samples stained with the Golgi method (Fischbach & Dittrich 1989, Ramón y Cajal & Sanchez 1915, Strausfeld 1971). This catalog was recently extended in large electron-microscopic data sets provided by the Janelia Research Campus (Takemura et al. 2013, 2017; Shinomiya et al. 2019). Within the optic lobe, the following general cell classes bear special relevance to the motion detection circuit (**Figure 2d**): Outer photoreceptors R1–R6 send their axons to the lamina where they contact large monopolar cells, called L1–L5 (Meinertzhagen & O'Neil 1991). The axons of lamina monopolar cells cross over in the first optic chiasm (**Figure 2c**) and convey the photoreceptor signals to layers 1–5 in the outer medulla. Medulla intrinsic (Mi) neurons connect the different layers of the medulla with each other. Transmedullary (Tm) neurons establish connections within the medulla and, in addition, connect specific layers of the medulla to the lobula or to both the lobula and the lobula plate. Centrifugal (C) neurons make connections in the medulla and the lamina. The complex tangential (CT) cell 1, despite innervating every single column of both the medulla and the lobula, contributes exclusively to local signal processing within each column (Meier & Borst 2019). Of special importance in the present context are the bushy T cells T4 and

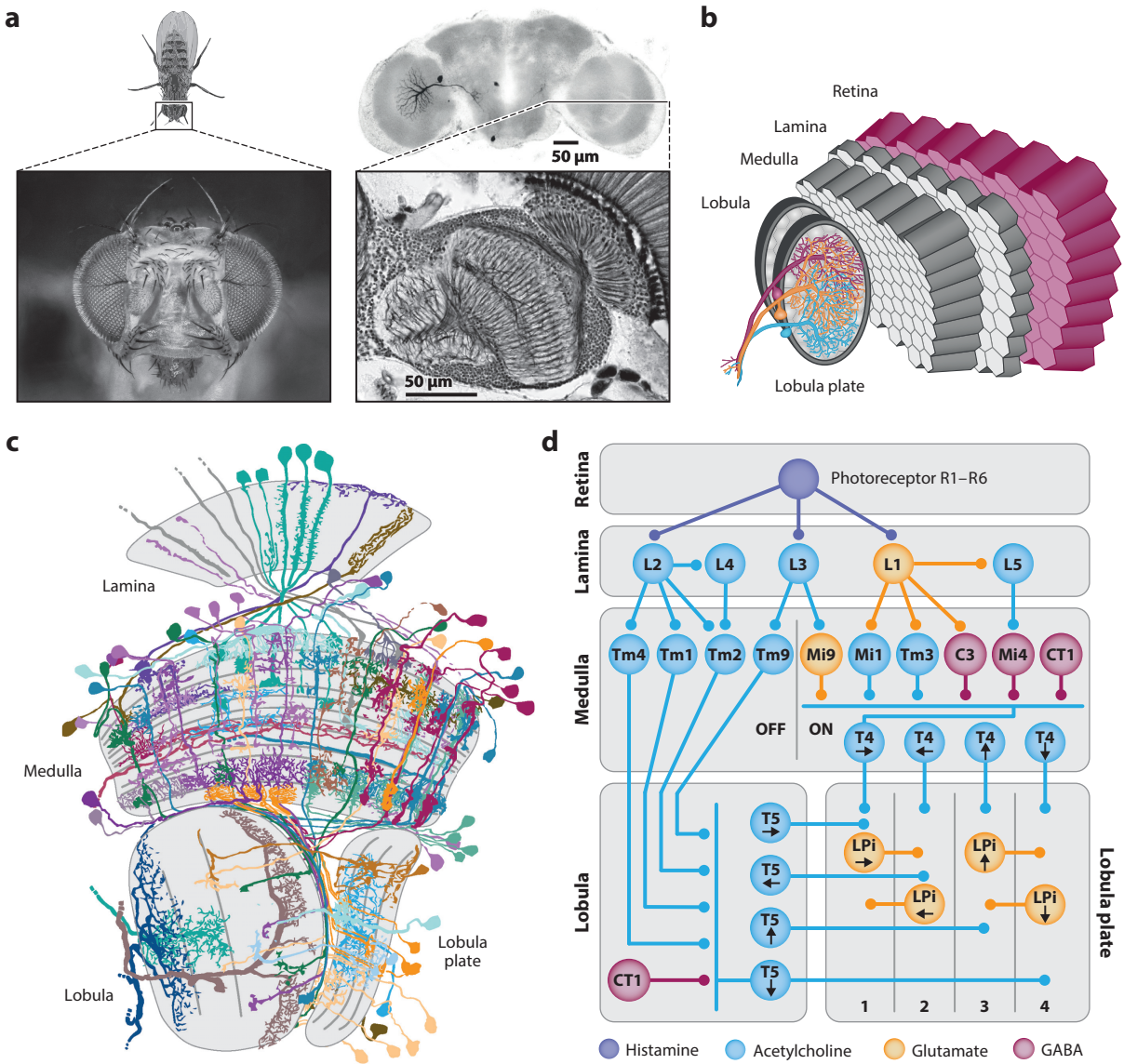


Figure 2

Anatomy of the fly optic lobe. (a) Micrograph of a *Drosophila* head with a facet eye on either side (left). (Right) Frontal cross section of a *Drosophila* brain with a single lobula plate tangential cell stained after a patch-clamp recording (top) and horizontal cross section of the optic lobe stained by Bodian's method, showing the columnar organization (bottom). Scale bars: 50 μm. Panel *a* adapted with permission from Takemura et al. (2008). Photo of the fly head provided by Florian Richter. (b) Schematic of the optic lobe. In the lobula plate, three tangential cells are shown. Panel *b* adapted with permission from Borst & Euler (2011). (c) Collection of different cell types in the *Drosophila* optic lobe. Panel *c* adapted with permission from Borst et al. (2020). (d) Schematic diagram of the motion vision circuit. Photoreceptors connect to lamina (L) cells that split signals into an ON and an OFF pathway. Transmedullary (Tm), medulla intrinsic (Mi), centrifugal (C), and complex tangential (CT) cells relay temporally filtered signals to the dendrites of T4 cells in the medulla and of T5 cells in the lobula. Different types of T4 and T5 cells send their axons to one out of four layers of the lobula plate, where they synapse onto lobula plate intrinsic (LPI) and lobula plate tangential cells (not shown). Some connections and cell types have been omitted for clarity.

T5 (see below), which connect the medulla (T4) and the lobula (T5) to the lobula plate, where they provide synaptic input to a broad range of small- and wide-field interneurons, including lobula plate tangential cells (Shinomiya et al. 2022). With its large dendrites (Cuntz et al. 2013), each tangential cell spans some hundreds of columns to receive input from T4 and T5 cells in one of the four layers of the lobula plate. By spatially integrating their input signals, these cells have large receptive fields (Krapp et al. 1998, Single & Borst 1998). Each tangential cell depolarizes in response to wide-field visual motion in one direction and hyperpolarizes in response to motion in the opposite direction (Bishop et al. 1968, Dvorak et al. 1975, Hausen 1976, Joesch et al. 2008). Their membrane potentials are tuned to specific types of optic flow. Horizontal system cells are tuned to horizontal motion (three of them are depicted in **Figure 2b**), and vertical system (VS) cells are tuned to vertical motion. The tangential cells' response properties broadly meet the criteria for the output of a Hassenstein–Reichardt detector (Egelhaaf et al. 1989, Haag et al. 2004), with the difference that the motion-opponent signals are not local but integrated over space.

ON and OFF Pathways

As an important characteristic of visual processing, just like in the mammalian retina (Schiller et al. 1986; for a review, see Borst & Helmstaedter 2015), the luminance signal is split into two pathways. The ON pathway carries information about luminance increments, whereas the OFF pathway signals luminance decrements. The costratification of different types of neurons in specific layers of the medulla and metabolic activity labeling with radioactive 2-deoxyglucose (Bausenwein & Fischbach 1992, Bausenwein et al. 1992) provided an early hint at the existence of parallel motion pathways in the fly, but their functional segregation remained a matter of speculation (Egelhaaf & Borst 1992). Only the ability to target and block specific lamina neurons genetically resolved this issue. Joesch et al. (2010) found that blocking the output of L1 reduces the responses of lobula plate tangential cells to moving ON edges, whereas blocking the output of L2 reduces responses to moving OFF edges. Behavioral (Clark et al. 2011) and electrophysiological studies (Eichner et al. 2011, Joesch et al. 2013) using different sequences of ON and OFF stimuli at adjacent image points confirmed the existence of two separate motion detectors. They respond to homotypic ON–ON and OFF–OFF, but not to heterotypic ON–OFF or OFF–ON, contrast changes at adjacent image points. More recent functional and structural studies demonstrate that lamina neurons L3 (Shinomiya et al. 2014, Silies et al. 2013) and L4 (Meier et al. 2014, Takemura et al. 2011, Tuthill et al. 2013) also feed into the OFF pathway. Together, these experiments suggest that the photoreceptor input is split into two parallel—albeit not symmetrical (Leonhardt et al. 2016)—streams of information that transmit signals about luminance increments (L1) and luminance decrements (L2–L4) separately to downstream motion detectors (**Figure 2d**).

T4 AND T5 CELLS

General Properties

T4 and T5 cells were first described by Ramón y Cajal & Sanchez (1915) as curious elements that generate bi-tufted stems (**Figure 3a**). The two cell types differ morphologically in the location of their dendritic tuft: T4 cells innervate layer 10 of the medulla, whereas T5 cells innervate layer 1 of the lobula (**Figure 3b**). T4 and T5 cells each come in four different subtypes per column (marked by the suffixes a, b, c, and d, respectively), the dendrites of which transcend column borders (**Figure 3c,d**). The axons of each of the four subtypes terminate in one out of the four layers of the lobula plate (Fischbach & Dittrich 1989) (**Figure 3b,d**). Since 2-deoxyglucose labeling indicated activity in separate layers depending on the direction of visual motion (Buchner et al. 1984), T4 and T5 cells, with their axonal projection pattern, were early candidates for local elementary motion

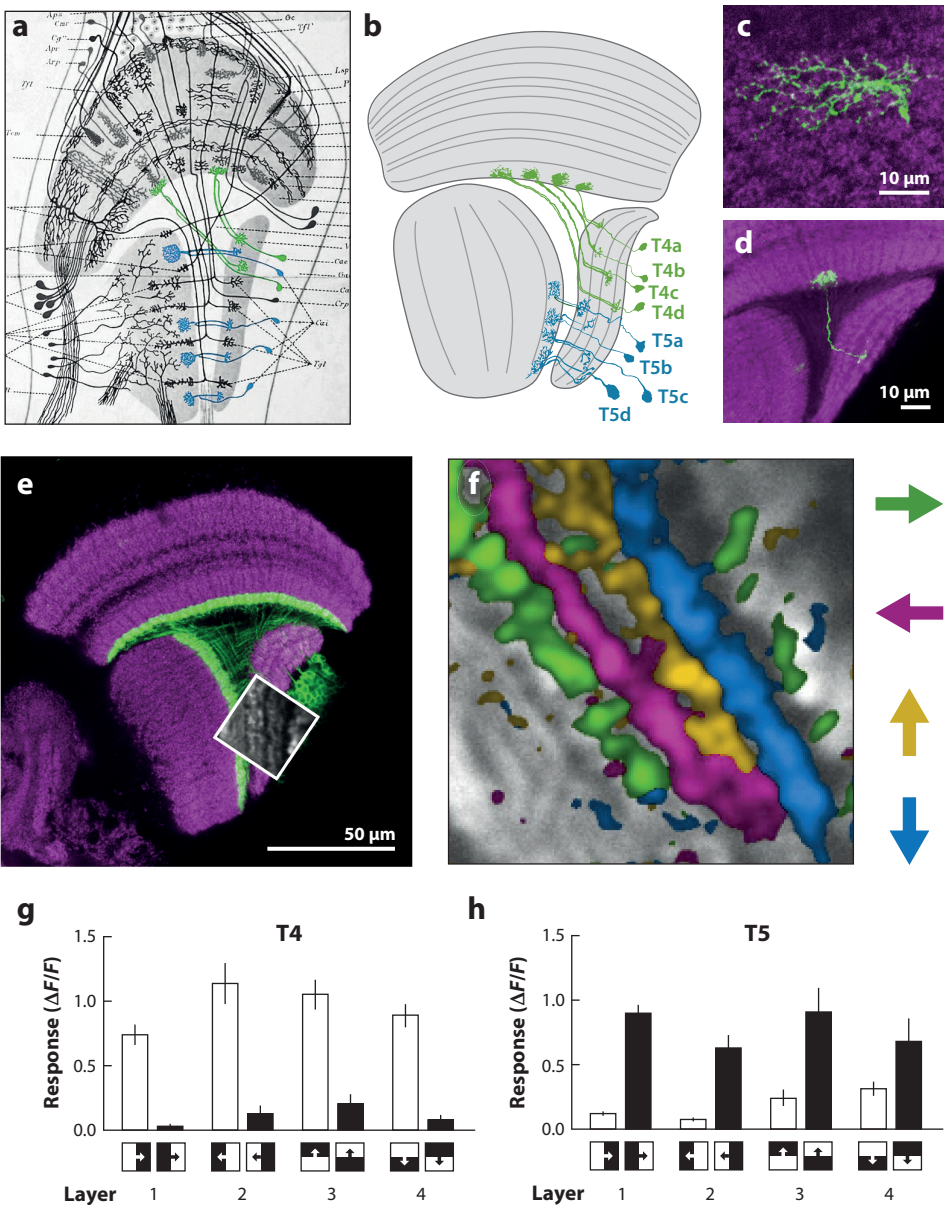


Figure 3

T4 and T5 cells as the primary motion-sensing neurons in the fly visual system. (a) First drawing of T4 and T5 cells. Panel *a* adapted from Ramón y Cajal & Sanchez (1915) (public domain). (b) Schematic of the four subtypes of T4 and T5 cells. Each subtype projects to one of the four layers of the lobula plate. Panel *b* adapted with permission from Fischbach & Dittrich (1989). (c,d) A single T4 neuron (green) extends its dendrite (*c*) across multiple medulla columns and sends its axon (*d*) to one of the four lobula plate layers. Micrographs in panels *c* and *d* provided by Jesús Pujol-Martí. (e) Confocal micrograph of the optic lobe with T4 and T5 cells labeled in green. Inset corresponds to image in panel *f*. Panel *e* adapted with permission from Groschner et al. (2022). (f) Calcium signals in T4/T5 axon terminals reveal four subtypes tuned to the four cardinal directions (*arrows*). The image is colorized according to the stimulus direction that elicits the strongest response. (g) T4 cells respond preferentially to moving ON edges. (h) T5 cells respond preferentially to moving OFF edges. Panels *f–h* adapted with permission from Maisak et al. (2013).

detectors. Their small sizes, however, frustrated initial attempts at electrophysiological recordings and left their visual response properties unknown for long. This problem was solved by the use of advanced gene expression systems (Brand & Perrimon 1993, Jenett et al. 2012, Pfeiffer et al. 2008) to target highly sensitive genetically encoded calcium indicators (Akerboom et al. 2012) specifically to T4 and T5 cells. Maisak et al. (2013) were the first to record direction-selective activity from T4 and T5 cells using two-photon calcium imaging while stimulating transgenic flies with gratings moving in the four cardinal directions (front-to-back, back-to-front, upward, and downward). Calcium signals in each of the four lobula plate layers encode a different direction (**Figure 3e,f**). Restricted expression of the calcium indicator in either T4 or T5 cells revealed the distinct contributions of the two cell types. While their response properties are similar with respect to the orientation and the velocity of moving gratings, they differ in their preferred contrast polarity (Maisak et al. 2013). T4 cells respond selectively to moving ON edges (**Figure 3g**), whereas T5 cells respond preferentially to moving OFF edges (Maisak et al. 2013, Fisher et al. 2015) (**Figure 3b**).

To test to what extent T4 and T5 cells inform postsynaptic lobula plate tangential cells on the one hand and visually guided behavior on the other, T4 and T5 cells were blocked genetically. The absence of synaptic transmission from T4 and T5 cells leads to a complete loss of motion responses in lobula plate tangential cells (Schnell et al. 2012), of the optomotor turning response of tethered walking flies (Bahl et al. 2013), of walking speed modulation by translational optic flow (Creamer et al. 2018), and of two types of looming-sensitive behavior: the landing and the avoidance response (Schilling & Borst 2015). In free flight, the straightness of the flies' trajectories is significantly reduced when T4 and T5 cells are blocked, comparable to that of control flies in complete darkness (Leonte et al. 2021). When asymmetry in propulsive forces is generated by unilateral wing clipping, control flies show a remarkable level of compensation, while flies whose T4 and T5 cells are blocked exhibit pronounced circling behavior (Leonte et al. 2021). Blocking T4 cells leads to a selective loss of responses to moving ON edges in the electrical activity of tangential cells as well as in optomotor behavior. Conversely, blocking T5 cells leads to a loss of responses to moving OFF edges in both assays (Maisak et al. 2013). In summary, the selective defects of flies with a T4 cell block for ON and flies with a T5 cell block for OFF edges corroborate the above findings concerning the selective responses of T4 and T5 cells to edges of different contrast polarity. The behavioral defects of flies with both T4 and T5 cells blocked suggest that these cells are indeed the primary motion-sensing neurons of the fly visual system, providing the major—if not the exclusive—directional inputs to downstream circuits and visual motion-driven behaviors. As tested so far, all information about the direction of visual motion seems to be lost when the collective output of T4 and T5 cells is blocked.

Input Organization

Volumetric electron microscopy of the *Drosophila* optic lobe provided two important insights (Takemura et al. 2017, Shinomiya et al. 2019): First, each of the four subtypes of T4 and T5 cells has a characteristic orientation of its dendrite within the respective retinotopically arranged neuropil (medulla for T4 cells and lobula for T5 cells). This orientation is such that the dendrite points with its extremely thin tips of less than 100 nm in diameter against the direction from which a stimulus moving along the cell's preferred direction would enter the cell's receptive field (**Figure 4a**). Second, on their dendrites, all subtypes of one cell type receive input from the same presynaptic partners but in a subtype-specific spatial arrangement (**Figure 4b**). Within the retinotopic coordinate system of the medulla, a cell of subtype T4a, sensitive to rightward motion, receives Mi9 input in the left column, Mi1 and Tm3 input in the central column, and Mi4, C3, and CT1 input in the right column. The corresponding member of subtype T4b, sensitive to leftward motion, receives Mi9 input in the right column, Mi1 and Tm3 input in the central column, and

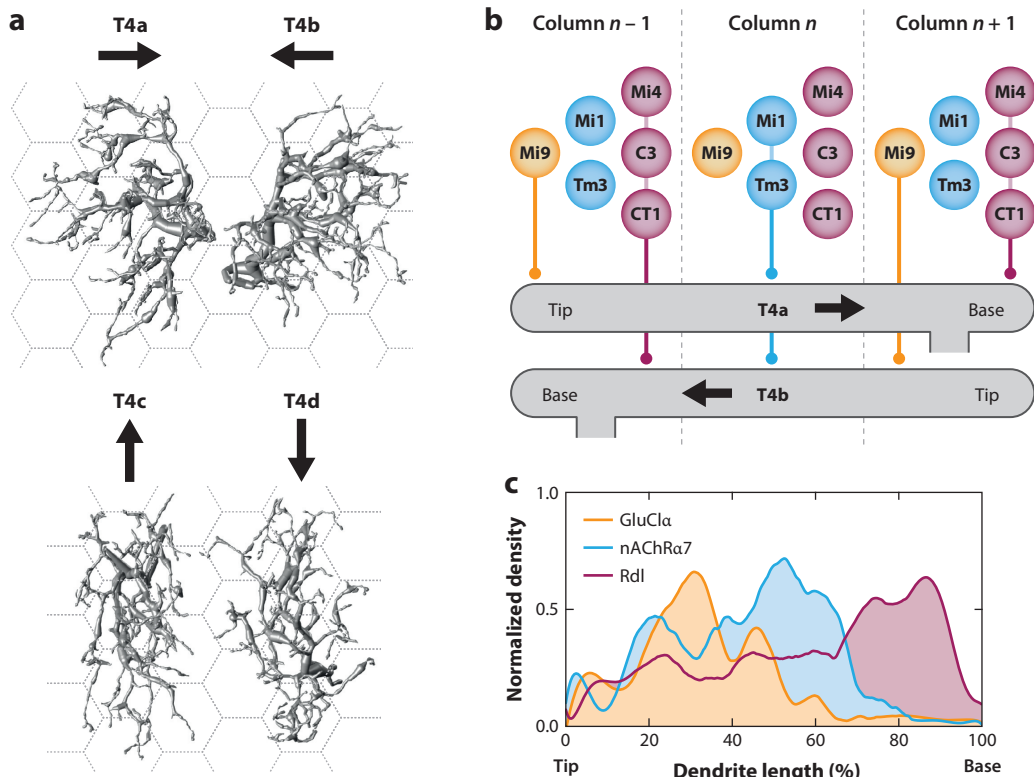


Figure 4

T4 cell dendrites are polarized according to their preferred direction. (a) Anatomical polarization. Electron microscopic reconstructions of the four T4 subtypes are shown (Shinomiya et al. 2019). Within the retinotopic map of the optic lobes, the tips of the dendrites are directed against the preferred direction (arrow) of each subtype. (b) Synaptic input polarization. T4 dendrites receive input from glutamatergic Mi9 in the column where they extend their tips, from cholinergic Mi1 and Tm3 in the central column, and from GABAergic Mi4, C3, and CT1 in the column where they enter, that is, the base of their dendrite. Panels *a* and *b* adapted from Shinomiya et al. (2019) (CC BY 4.0). (c) Transmitter receptor distribution. Across all subtypes, the glutamate-gated chloride channel GluCl α is found primarily at the dendritic tips, the nicotinic acetylcholine receptor nAChR $\alpha 7$ is found at the center, and the GABA receptor Rdl is found at the base of the dendrite. Data for panel *c* from Fendl et al. (2020). Abbreviations: C, centrifugal; CT, complex tangential; GABA, γ -aminobutyric acid; GluCl α , glutamate-gated chloride channel α ; Mi, medulla intrinsic; nAChR $\alpha 7$, nicotinic acetylcholine receptor $\alpha 7$; Rdl, resistant to dieldrin; Tm, transmedullary.

Mi4, C3, and CT1 input in the left column. The same is true for subtypes T4c and T4d, just with respect to the upper and lower columns.

Immunohistochemical studies (Pankova & Borst 2017, Richter et al. 2018, Takemura et al. 2017) identified the transmitter phenotype of each input neuron, which has important implications for the functional interpretation of this input organization. Together with single-cell RNA sequencing (Davis et al. 2020), these studies revealed that Mi9 uses glutamate, Mi1 and Tm3 use acetylcholine, and Mi4, C3, and CT1 use γ -aminobutyric acid (GABA) as their respective transmitters. To understand the effect of a transmitter on the postsynaptic neuron, the respective receptor is of decisive importance. Single-cell and bulk RNA sequencing in T4 cells showed high expression levels of the glutamate-gated chloride channel GluCl α and several subunits of nicotinic acetylcholine and GABA_A receptors (Davis et al. 2020, Hörmann et al. 2020, Pankova & Borst 2016). Using a novel method for the conditional tagging of endogenous proteins,

Fendl et al. (2020) visualized the spatial distribution of the corresponding neurotransmitter receptors on single T4 cell dendrites. They found GluCl α channels at the distal tips of the T4 dendrite, nicotinic acetylcholine receptors at the center, and GABA A receptors at the base of the dendrite (**Figure 4c**). This spatial distribution quantitatively matches that of the synapses formed by Mi9 cells at the tips, by Mi1 and Tm3 at the center, and by Mi4, C3, and CT1 cells at the base (Shinomiya et al. 2019, Takemura et al. 2017).

T5 cells show similar wiring specificity. Adhering to the columnar boundaries of the lobula, a T5 dendrite samples from Tm9 cells in the distal column, from Tm1, Tm2, and Tm4 cells in the central column, and from CT1 in the proximal column. In contrast to the diverse neurotransmitters released by the presynaptic partners of T4 cells, the inputs to T5 dendrites are almost exclusively cholinergic. CT1 is the only GABAergic exception (Shinomiya et al. 2014, 2019).

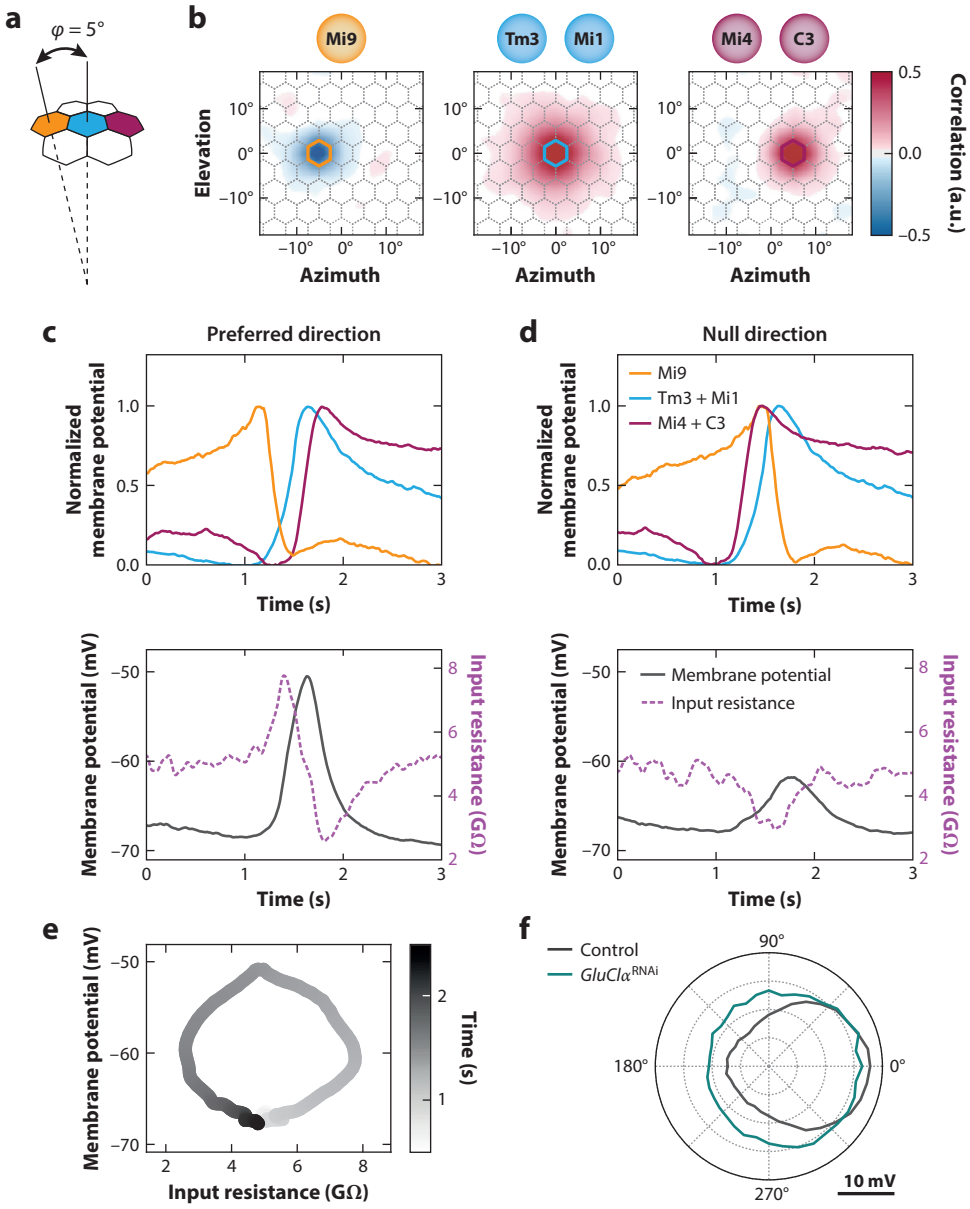
Besides its functional implications (see below), the input organization outlined above poses a most interesting problem for the development of T4 and T5 cells, which originate from common progenitors through a subtype-specific combination of transcription factors (Apitz & Salecker 2018, Pinto-Teixeira et al. 2018): How can a T4 cell know from which input neuron to sample depending on the exact column it extends its dendrite into and on the exact subtype it represents? Or seen from the perspective of a presynaptic columnar neuron, how can this cell, confronted with the dendrites of 12 different T4 cells (tips, center, and base from all four subtypes), decide which cell to contact and which to avoid? This problem cannot be solved by subtype-specific receptor expression, since all subtypes receive input from precisely the same set of medulla neurons. One idea comes from the observation that the spatial connectivity pattern of all subtypes with respect to their cell-intrinsic coordinates is identical. All T4 subtypes reveal the same pattern of connectivity with Mi9 cells at the tips, with Mi1 and Tm3 at the center, and with Mi4, C3, and CT1 cells at the base of the dendrite. Then, the decisive factor in development that distinguishes subtype T4a from subtype T4b, and so on, is the spatial orientation of the dendrite. In support of this hypothesis, Hörmann et al. (2020) and Kurmangaliyev et al. (2019) found the transcription factor *grain* to be expressed only in subtypes T4b and T4c, that is, in T4 cells tuned to back-to-front and upward motion, respectively. Overexpression of *grain* in all T4 cells resulted in a T4 population consisting only of subtypes T4b and T4c, including the correct dendrite orientation and functional properties. The opposite was found in *grain* knock-down experiments, where the transcription factor was removed from all subtypes, resulting in subtypes T4a and T4d only (Hörmann et al. 2020). These experiments suggest that dendrite orientation is the decisive step in development that distinguishes the different subtypes from each other. Once this is accomplished, connectivity follows for all subtypes according to the same rules.

Biophysical Mechanisms of Direction Selectivity

The clear tripartite organization of presynaptic neurons and postsynaptic receptors on T4 dendrites (**Figures 4b,c** and **5a**) provides a hint at how the proposed three-arm motion detector (Haag et al. 2016, Leong et al. 2016) (**Figure 1e**) might take biological form. But to turn the algorithmic formalism into a biophysically plausible model of how T4 and T5 cells compute, it is necessary to consider not just their direction-selective output but also their nondirectional input signals. Genetic access to the input elements allowed for the cataloging of spatial and temporal response properties of the medullary input neurons and provided three important insights: First, in the stream of visual information, differential ON and OFF responses to different contrast polarities first appear in the medulla (Behnia et al. 2014, Meier et al. 2014, Strother et al. 2014). Second, most medullary neurons adjust their sensitivity to the prevailing image contrast to guarantee adequate signal amplitudes over a wide range of contrast values (Drews et al. 2020, Matulis et al. 2020).

And third, in agreement with the Hassenstein-Reichardt model, medullary neurons constitute a temporal filter bank that supplies both T4 and T5 cells with a repertoire of differentially filtered input signals (Arenz et al. 2017, Serbe et al. 2016, Strother et al. 2017, Yang et al. 2016).

In the OFF pathway, Tm9 neurons, which form synapses at the tips of T5 dendrites, have much longer response time constants compared to those of Tm1, Tm2, and Tm4 in the neighboring column (Serbe et al. 2016). Consequently, an enhancement of responses to motion in the preferred direction could arise from a supralinear interaction between the excitatory synapses in the two columns (Leong et al. 2016, Haag et al. 2017). Responses to motion in the null direction



(Caption appears on following page)

Figure 5 (Figure appears on preceding page)

Multiplicative disinhibition in T4 cells. (a) The angle ϕ between the optical axes of two adjacent ommatidia amounts to approximately 5° in *Drosophila*. (b) Spatial organization of T4 input neurons with respect to the hexagonal retinotopic grid. A T4 cell receives input from Mi9 in the left column (yellow), from Tm3 and Mi1 in the central column (blue), and from Mi4 and C3 in the right column (magenta). Heatmaps show the average spatial receptive fields of the input cells determined by reverse correlation of changes in membrane potential and local luminance in a white-noise stimulus. Note the negative correlation for Mi9. (c,d) Temporal sequence of input signals (top), T4 membrane potential (solid line, bottom), and T4 input resistance (dashed line, bottom) in response to an ON edge moving in the preferred (c) or in the null (d) direction of the T4 cell. (e) T4 input resistance as a function of membrane potential and time for data in panel c. (f) Directional tuning curves of T4 neurons with (dark gray) and without (teal) the inhibitory glutamate receptor GluCl α . Panels b–f adapted from Groschner et al. (2022). Abbreviations: C, centrifugal; GluCl α , glutamate-gated chloride channel α ; Mi, medulla intrinsic; Tm, transmedullary.

are suppressed through spatially offset inhibition (Gruntman et al. 2019), whose likely source is the amacrine cell CT1 that forms synapses at the base of the T5 dendrite (Meier & Borst 2019, Shinomiya et al. 2019).

In the ON pathway, the correspondence between the circuit architecture and the three-arm model is even more clear-cut. The signals of Mi1 and Tm3 in the central arm are fast; those of the main flanking neurons, Mi9 and Mi4, are slow (Arenz et al. 2017). The GABAergic neurons Mi4, C3, and CT1 likely account for the suppression of T4 responses to motion in the null direction (Gruntman et al. 2018). The glutamatergic neuron Mi9 stands out due to the polarity of its response. While the signals of all other T4 input elements are positively correlated with changes in luminance—as expected from cells in the ON pathway—those of Mi9 neurons are anticorrelated (Arenz et al. 2017, Strother et al. 2017) (Figure 5b). Mi9 neurons act on T4 cells through the inhibitory glutamate receptor GluCl α (Cully et al. 1996, Davis et al. 2020, Liu & Wilson 2013, Pankova & Borst 2016), which suggests a twofold sign inversion: the release from inhibition upon luminance increment. This hypothesis posits Mi9 as the source of continuous shunting inhibition (Borst 2018). During ON-edge motion in the preferred direction of a T4 cell, when the receptive field of Mi9 is stimulated by light, slow disinhibition is predicted to coincide with fast excitation from the adjacent column and amplify the response multiplicatively (Borst 2018, Koch & Poggio 1992). A stimulus moving in the null direction would first set off a slow inhibitory signal from Mi4 and C3 neurons that cancels out the subsequent excitation. This model and variants thereof reproduced many aspects of T4 cell activity (Badwan et al. 2019, Borst 2018, Zavatone-Veth et al. 2020) but lacked a firm experimental basis until recently.

Multiplicative Disinhibition

The renaissance of whole-cell patch-clamp recordings from small neurons in the optic lobe of *Drosophila* (Behnia et al. 2014, Gruntman et al. 2018) prompted a thorough electrophysiological investigation of the above model (Groschner et al. 2022). Membrane potential measurements from postsynaptic T4 cells and from their presynaptic partners revealed the well-orchestrated temporal sequence of input signals as it unfolds during motion in the preferred (Figure 5c) and in the null direction of the T4 cell (Figure 5d). In the latter case, the slow flanking inputs cover the central excitatory input in a seamless blanket of inhibition. During motion in the preferred direction, however, excitation coincides with a transient release from inhibition that amplifies the response multiplicatively through an increase in postsynaptic resistance (Borst 2018, Groschner et al. 2022, Koch & Poggio 1992). The input resistance of the T4 cell changes along a circular trajectory as a function of the membrane potential (Figure 5e), where the peak in resistance precedes the peak in membrane potential. This dynamic depends on the direction of visual motion as well as on the

presence of GluCl α (Groschner et al. 2022). In the absence of the glutamate receptor, that is, in the absence of input from Mi9, T4 neurons are trapped in a state of high excitability and respond strongly to visual motion not just in one direction but in many (**Figure 5f**). Elegant and simple as this passive disinhibitory mechanism might be, there are in all likelihood additional nonlinearities that shape the responses of T4 cells. A nonlinear voltage-to-calcium transformation, for example, further sharpens the directional tuning curve of T4 and T5 cells (Mishra et al. 2022, Wienecke et al. 2018).

MOTION OPPONENTY BY LOBULA PLATE INTRINSIC CELLS

The depolarization of a lobula plate tangential cell in response to visual motion in their preferred direction is readily explained by cholinergic excitation from those T4/T5 cells, which project to the same lobula plate layer as the tangential cell's dendrite. The hyperpolarizing response to motion in the null direction, however, entails a sign inversion, which could come from a second, inhibitory population of elementary motion detectors. Two pieces of evidence speak against this possibility: First, blocking the synaptic output of T4/T5 cells abolishes all tangential cell responses, regardless of their polarity (Schnell et al. 2012). Second, optogenetic activation of T4/T5 cells evokes a biphasic postsynaptic potential in tangential cells, which consists of a fast excitatory and a slow inhibitory component (Mauss et al. 2014). These findings suggest, in addition to the direct excitation, an inhibitory feedforward connection between T4/T5 cells and tangential cells of opposite preferred direction. The juxtaposition of lobula plate layers with opposite directional preferences (**Figure 3f**) implies that such an inhibitory element needs to innervate two adjacent layers (Mauss et al. 2014). Bistratified neurons that fit this description were discovered by Mauss et al. (2015) and dubbed lobula plate intrinsic (LPI) interneurons. Collectively, they tile the retinotopic map of the lobula plate (**Figure 6a**), where they overlap with the extensive dendrites of tangential cells (**Figure 6b**). Each LPI cell ramifies within two out of the four layers defined by the axon terminals of T4/T5 cells but shows presynaptic specializations in only one of them (**Figure 6c**). Optogenetic stimulation of LPI₃₋₄ cells (with presynapses in layer 4) causes a fast inhibitory postsynaptic potential in VS cells of layer 4 that scales with stimulus intensity (**Figure 6d**). Calcium imaging experiments revealed that LPI cells are directionally selective and share their preferred direction with those T4/T5 cells that terminate in their postsynaptic layer (**Figure 6e**). Silencing LPI cells prevents the hyperpolarizing response of tangential cells during null-direction motion but leaves their depolarizing response to preferred-direction motion unaffected (**Figure 6f**). The experiments described above demonstrate that LPI cells receive excitation from T4/T5 cells in one layer and forward an inhibitory signal to the neighboring, oppositely tuned layer. It follows that downstream tangential cells receive two types of local direction-selective input: direct excitation from T4 and T5 cells in their jointly innervated lobula plate layer and indirect inhibition from LPI cells activated by T4/T5 terminals in the neighboring layer. The latter is mediated, again, by the expression of GluCl α (Mauss et al. 2015, Richter et al. 2018).

Looking back onto the original Hassenstein-Reichardt model, its neural implementation seems more parsimonious and differs in the following way: First, the subtraction occurs on the dendrites simultaneously with spatial integration of directional motion information (Borst & Egelhaaf 1990, Egelhaaf et al. 1989). Second, instead of repeating the computation of a certain direction for its use as an inhibitory signal, this computation is done only once and subsequently converted into an inhibitory signal in the adjacent lobula plate layer via LPI neurons (Mauss et al. 2015). What might be the functional relevance of this subtractive processing stage? Originally, the subtraction of opponent subunits was thought to improve the rather low direction selectivity of a

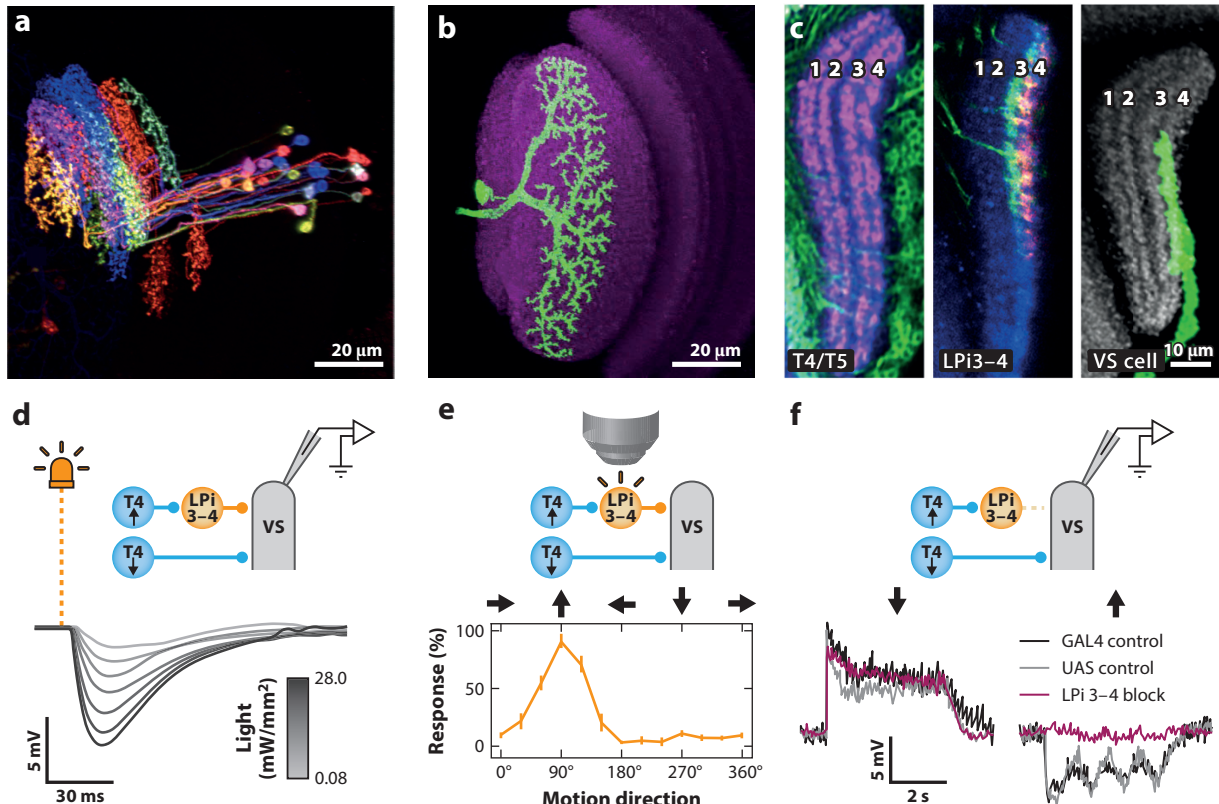


Figure 6

Lobula plate intrinsic (LPI) neurons create motion opponency in lobula plate tangential cells. (a) Multicolor flip-out showing several individual LPI neurons tiling the lobula plate in retinotopic space. Micrograph provided by Aljoscha Nern. (b) Frontal view of the lobula plate with a fluorescently labeled vertical system (VS) cell (green). (c, left) Horizontal cross section of the lobula plate, with T4/T5 cells expressing green fluorescent protein (GFP) (green) and presynaptic synaptotagmin-HA (red) in the axon terminals of the four layers. (Middle) LPi3-4 neurons expressing GFP (green) and presynaptic synaptotagmin-HA (red). Neurons ramify in layers 3 and 4 but have presynaptic specializations restricted to layer 4 only. (Right) A VS cell with downward direction selectivity extends its dendrite to layer 4. (d) VS cells in layer 4 hyperpolarize in response to optogenetic activation (2 ms, dashed line) of LPi3-4 neurons with different light intensities (grayscale). (e) Two-photon calcium imaging revealed that LPi3-4 neurons respond preferentially to upward motion, as do T4c and T5c cells terminating in layer 3. (f) Visually evoked membrane potential responses of VS cells with and without input from LPI neurons. Blocking LPI cells by LPi3-4-specific expression of the transcription factor GAL4 in combination with a tetanus toxin light-chain transgene under control of the upstream activating sequence (UAS) leaves the depolarizing preferred-direction response of a VS cell unaffected (left, red) but abolishes its hyperpolarizing null-direction response (right, red). In flies that carry either of the transgenes in isolation, VS cells exhibit fully motion-opponent responses (GAL4 control, black; UAS control, gray). Panels b–f adapted with permission from Mauss et al. (2015).

single subunit of the Hassenstein–Reichardt detector (Borst & Egelhaaf 1990, Single et al. 1997). In the fly, however, this seems unnecessary since T4/T5 cells already deliver a narrowly tuned direction-selective signal (Haag et al. 2016, Maisak et al. 2013). Due to their large receptive fields, lobula plate tangential cells are well suited to detect optic flow arising from self-motion (Krapp & Hengstenberg 1996, Krapp et al. 2001). Depending on the maneuver, flow fields may be unidirectional, as experienced during rotation about the left-right body axis, or they may be dominated by expansion, as occurring during forward translation. Recordings from VS cells show that they are predominantly depolarized by unidirectional (downward) and not by expanding flow fields.

Genetically silencing the LPi cells strongly impairs this selectivity: Tangential cells now respond unselectively to a motion noise and expansion flow field (Mauss et al. 2015). Under normal conditions, the tangential cells' reduced responses to such stimuli are explained by response cancelation of opponent inputs impinging on different parts of the dendrite. Motion-opponent subtraction therefore seems essential for flow-field selectivity in wide-field motion-sensitive neurons.

REMAINING QUESTIONS

The past decade has seen enormous progress in our understanding of the motion vision circuitry in the fruit fly *Drosophila*. Given that only 13 years ago ON and OFF channels were unknown in flies and T4/T5 cell function was only the subject of speculation, the present picture is much clearer and contains rich detail concerning the cells involved, their connectivity, and their response properties. The neurobiological implementations of the three main processing steps of the Hassenstein–Reichardt detector (temporal filtering, multiplication, and subtraction) have been identified, at least in the ON motion pathway. Nonetheless, we are still missing answers to a number of important questions.

One question concerns the biophysical mechanism underlying preferred direction enhancement in T5 cells. Unlike T4 cells, T5 cells receive almost exclusive cholinergic input from Tm9 on the preferred side of their dendrite and from Tm1, Tm2, and Tm4 in the central part. A single inhibitory input is provided from the wide-field amacrine cell CT1 on the null side. With all input neurons having OFF center receptive fields (Kohn et al. 2021, Meier & Borst 2019, Serbe et al. 2016), a disinhibitory mechanism like the one described for T4 cells (Groschner et al. 2022) can be ruled out. Further experiments are needed to reveal the mechanism by which the slow signals of Tm9 can amplify the subsequent fast excitation a T5 cell receives from Tm1, Tm2, and Tm4.

Another unanswered question is that of how two neurons of virtually identical morphology (Shinomiya et al. 2019) can transmit signals with vastly different temporal dynamics (Arenz et al. 2017, Serbe et al. 2016). In other words, what makes a neuron a low-pass or a band-pass filter? The differential expression of ion channels, while doubtlessly important (Gonzalez-Suarez et al. 2022), seems to account only partially for the temporal filter properties of medullary neurons. Recurrent connections within the medulla or synaptic mechanisms might contribute to delaying the signal of one neuron relative to that of its neighbor as well.

An even broader question concerns the seemingly redundant inputs to T4 and T5 cells. Connectomic analyses identified more presynaptic partners of T4 and T5 cells than actually needed, given the general computational structure of the three-arm detector. Instead of three input cells, both T4 and T5 cells receive synaptic input from seven different cells, including T4 and T5 cells of the same preferred direction. What is the specific function of each of these inputs? In the case of Mi1 and Tm3, both providing excitatory input to the center part of the T4 dendrite, this question has been answered by demonstrating that these inputs are specialized with respect to different velocity regimes (Ammer et al. 2015). This conclusion has been reached after blocking each input selectively and probing the deficit in the edge response of tangential cells at various velocities. However, the interpretation of such blocking experiments is complicated by the fact that each of the input neurons, in addition to its synapses onto T4 or T5 cells, also connects to other input neurons, either directly or indirectly (Shinomiya et al. 2019). These network interactions change the response characteristics of the other inputs onto T4 and T5 cells as well, making clear conclusions concerning the specific impact of the blocked input neuron for the T4 or T5 response difficult. What is needed here is a method that blocks the specific synapses from the input neuron onto T4 and T5 cells without affecting all the other output synapses of this cell. While such a method is not available at present, we can confine blocking experiments to the situation where

one input neuron uses a certain neurotransmitter exclusively and knock down the respective receptor in the postsynaptic T4 cell, like GluCl α for Mi9 input to T4 cells (Groschner et al. 2022), or resort to computer simulations.

DISCLOSURE STATEMENT

The authors are not aware of any affiliations, memberships, funding, or financial holdings that might be perceived as affecting the objectivity of this review.

ACKNOWLEDGMENTS

A.B. acknowledges the support of the Max Planck Society. L.N.G. acknowledges the support of the European Union's Horizon 2020 program under the Marie Skłodowska-Curie Action MOVIS grant agreement no. 896143.

LITERATURE CITED

- Ache JM, Polsky J, Alghailani S, Parekh R, Breads P, et al. 2019. Neural basis for looming size and velocity encoding in the *Drosophila* giant fiber escape pathway. *Curr. Biol.* 29(6):1073–81
- Akerboom J, Chen TW, Wardill TJ, Tian L, Marvin JS, Mutlu S, et al. 2012. Optimization of a GCaMP calcium indicator for neural activity imaging. *J. Neurosci.* 32(40):13819–40
- Ammer G, Leonhardt A, Bahl A, Dickson BJ, Borst A. 2015. Functional specialization of neural input elements to the *Drosophila* ON motion detector. *Curr. Biol.* 25(17):2247–53
- Apitz H, Salecker I. 2018. Spatio-temporal relays control layer identity of direction-selective neuron subtypes in *Drosophila*. *Nat. Commun.* 9(1):2295
- Arenz A, Drews MS, Richter FG, Ammer G, Borst A. 2017. The temporal tuning of the *Drosophila* motion detectors is determined by the dynamics of their input elements. *Curr. Biol.* 27(7):929–44
- Badwan BA, Creamer MS, Zavatone-Veth JA, Clark DA. 2019. Dynamic nonlinearities enable direction opponency in *Drosophila* elementary motion detectors. *Nat. Neurosci.* 22(8):1318–26
- Bahl A, Ammer G, Schilling T, Borst A. 2013. Object tracking in motion-blind flies. *Nat. Neurosci.* 16(6):730–38
- Barlow HB, Levick WR. 1965. The mechanism of directionally selective units in rabbit's retina. *J. Physiol.* 178(3):477–504
- Bausenwein B, Dittrich APM, Fischbach K-F. 1992. The optic lobe of *Drosophila melanogaster*. II. Sorting of retinotopic pathways in the medulla. *Cell Tissue Res.* 267(1):17–28
- Bausenwein B, Fischbach K-F. 1992. Activity labeling patterns in the medulla of *Drosophila melanogaster* caused by motion stimuli. *Cell Tissue Res.* 270(1):25–35
- Behnia R, Clark DA, Carter AG, Clandinin TR, Desplan C. 2014. Processing properties of ON and OFF pathways for *Drosophila* motion detection. *Nature* 512(7515):427–30
- Bishop LG, Keehn DG, McCann GD. 1968. Motion detection by interneurons of optic lobes and brain of the flies *Calliphora phaenia* and *Musca domestica*. *J. Neurophysiol.* 31(4):509–25
- Borst A. 2014. Fly visual course control: behaviour, algorithms and circuits. *Nat. Rev. Neurosci.* 15(9):590–99
- Borst A. 2018. A biophysical mechanism for preferred direction enhancement in fly motion vision. *PLOS Comput. Biol.* 14(6):e1006240
- Borst A, Bahde S. 1986. What kind of movement detector is triggering the landing response of the housefly? *Biol. Cybern.* 55(1):59–69
- Borst A, Drews M, Meier M. 2020. The neural network behind the eyes of a fly. *Curr. Opin. Physiol.* 16:33–42
- Borst A, Egelhaaf M. 1989. Principles of visual motion detection. *Trends Neurosci.* 12(8):297–306
- Borst A, Egelhaaf M. 1990. Direction selectivity of fly motion-sensitive neurons is computed in a two-stage process. *PNAS* 87(23):9363–67
- Borst A, Euler T. 2011. Seeing things in motion: models, circuits, and mechanisms. *Neuron* 71(6):974–94
- Borst A, Helmstaedter M. 2015. Common circuit design in fly and mammalian motion vision. *Nat. Neurosci.* 18(8):1067–76

- Brand AH, Perrimon N. 1993. Targeted gene expression as a means of altering cell fates and generating dominant phenotypes. *Development* 118(2):401–15
- Buchner E. 1976. Elementary movement detectors in an insect visual system. *Biol. Cybern.* 24(2):86–101
- Buchner E, Buchner S, Bülfhoff I. 1984. Deoxyglucose mapping of nervous activity induced in *Drosophila* brain by visual movement. *J. Comp. Physiol. A* 155:471–83
- Clark DA, Bursztyn L, Horowitz MA, Schnitzer MJ, Clandinin TR. 2011. Defining the computational structure of the motion detector in *Drosophila*. *Neuron* 70(6):1165–77
- Creamer MS, Mano O, Clark DA. 2018. Visual control of walking speed in *Drosophila*. *Neuron* 100(6):1460–73
- Cully DF, Paress PS, Liu KK, Schaeffer JM, Arena JP. 1996. Identification of a *Drosophila melanogaster* glutamate-gated chloride channel sensitive to the antiparasitic agent avermectin. *J. Biol. Chem.* 271(33):20187–91
- Cuntz H, Forstner F, Schnell B, Ammer G, Raghu SV, Borst A. 2013. Preserving neural function under extreme scaling. *PLOS ONE* 8(8):e71540
- Davis FP, Nern A, Picard S, Reiser MB, Rubin GM, et al. 2020. A genetic, genomic, and computational resource for exploring neural circuit function. *eLife* 9:e50901
- Drews MS, Leonhardt A, Pirogova N, Richter FG, Schuetzenberger A, et al. 2020. Dynamic signal compression for robust motion vision in flies. *Curr. Biol.* 30(2):209–21
- Dvorak DR, Bishop LG, Eckert HE. 1975. On the identification of movement detectors in the fly optic lobe. *J. Comp. Physiol.* 100(1):5–23
- Egelhaaf M, Borst A. 1992. Are there separate ON- and OFF-channels in fly motion vision? *Vis. Neurosci.* 8(2):151–64
- Egelhaaf M, Borst A, Reichardt W. 1989. Computational structure of a biological motion detection system as revealed by local detector analysis in the fly's nervous system. *J. Opt. Soc. Am. A* 6(7):1070–87
- Eichner H, Joesch M, Schnell B, Reiff DF, Borst A. 2011. Internal structure of the fly elementary motion detector. *Neuron* 70(6):1155–64
- Exner S. 1894. *Entwurf zu einer physiologischen Erklärung der psychischen Erscheinungen. I. Theil.* Vienna: Deuticke-Verlag
- Fendl S, Vieira RM, Borst A. 2020. Conditional protein tagging methods reveal highly specific subcellular distribution of ion channels in motion-sensing neurons. *eLife* 9:e62953
- Fenk LM, Avritzer SC, Weisman JL, Nair A, Randt LD, et al. 2022. Muscles that move the retina augment compound eye vision in *Drosophila*. *Nature* 612:116–22
- Fischbach K-F, Dittrich APM. 1989. The optic lobe of *Drosophila melanogaster*. I. A Golgi analysis of wild-type structure. *Cell Tissue Res.* 258:441–75
- Fisher YE, Silies M, Clandinin TR. 2015. Orientation selectivity sharpens motion detection in *Drosophila*. *Neuron* 88(2):390–402
- Gonzalez-Suarez AD, Zavatone-Veth JA, Chen J, Maulis CA, Badwan BA, Clark DA. 2022. Excitatory and inhibitory neural dynamics jointly tune motion detection. *Curr. Biol.* 32(17):3659–75.e8
- Götz K. 1964. Optomotorische Untersuchung des visuellen Systems einiger Augenmutanten der Fruchtfliege *Drosophila*. *Kybernetik* 2(2):77–92
- Groschner LN, Malis JG, Zuidinga B, Borst A. 2022. A biophysical account of multiplication by a single neuron. *Nature* 603(7899):119–23
- Gruntman E, Romani S, Reiser MB. 2018. Simple integration of fast excitation and offset, delayed inhibition computes directional selectivity in *Drosophila*. *Nat. Neurosci.* 21(2):250–57
- Gruntman E, Romani S, Reiser MB. 2019. The computation of directional selectivity in the *Drosophila* OFF motion pathway. *eLife* 8:e50706
- Haag J, Arenz A, Serbe E, Gabbiani F, Borst A. 2016. Complementary mechanisms create direction selectivity in the fly. *eLife* 5:e17421
- Haag J, Denk W, Borst A. 2004. Fly motion vision is based on Reichardt detectors regardless of the signal-to-noise ratio. *PNAS* 101(46):16333–38
- Haag J, Mishra A, Borst A. 2017. A common directional tuning mechanism of *Drosophila* motion-sensing neurons in the ON and in the OFF pathway. *eLife* 6:e29044
- Harris WA, Stark WS, Walker JA. 1976. Genetic dissection of the photoreceptor system in the compound eye of *Drosophila melanogaster*. *J. Physiol.* 256(2):415–39

- Hassenstein B, Reichardt W. 1956. Systemtheoretische Analyse der Zeit-, Reihenfolgen- und Vorzeichenauswertung bei der Bewegungsperception des Rüsselkäfers *Chlorophanus*. *Z. Naturforsch. B* 11:513–24
- Hausen K. 1976. Functional characterization and anatomical identification of motion sensitive neurons in the lobula plate of the blowfly *Calliphora erythrocephala*. *Z. Naturforsch. C* 31(9–10):629–34
- Heisenberg M, Buchner E. 1977. The role of retinula cell types in visual behavior of *Drosophila melanogaster*. *J. Comp. Physiol. A* 117:127–62
- Hindmarsh Sten T, Li R, Otopalik A, Ruta V. 2021. Sexual arousal gates visual processing during *Drosophila* courtship. *Nature* 595(7868):549–53
- Hörmann N, Schilling T, Haji Ali A, Serbe E, Mayer C, et al. 2020. A combinatorial code of transcription factors specifies subtypes of visual motion-sensing neurons in *Drosophila*. *Development* 147:dev186296
- Jenett A, Rubin GM, Ngo T-TB, Shepherd D, Murphy C, et al. 2012. A GAL4-driver line resource for *Drosophila* neurobiology. *Cell Rep.* 2(4):991–1001
- Joesch M, Plett J, Borst A, Reiff DF. 2008. Response properties of motion-sensitive visual interneurons in the lobula plate of *Drosophila melanogaster*. *Curr. Biol.* 18(5):368–74
- Joesch M, Schnell B, Raghu S, Reiff DF, Borst A. 2010. ON and OFF pathways in *Drosophila* motion vision. *Nature* 468(7321):300–4
- Joesch M, Weber F, Eichner H, Borst A. 2013. Functional specialization of parallel motion detection circuits in the fly. *J. Neurosci.* 33(3):902–5
- Koch C, Poggio T. 1992. Multiplying with synapses and neurons. In *Single Neuron Computation*, ed. T McKenna, J Davis, SF Zornetzer, pp. 315–45. San Diego: Academic
- Kohn JR, Portes JP, Christenson MP, Abbott LF, Behnia R. 2021. Flexible filtering by neural inputs supports motion computation across states and stimuli. *Curr. Biol.* 31(23):5249–60
- Krapp HG, Hengstenberg B, Hengstenberg R. 1998. Dendritic structure and receptive-field organization of optic flow processing interneurons in the fly. *J. Neurophysiol.* 79(4):1902–17
- Krapp HG, Hengstenberg R. 1996. Estimation of self-motion by optic flow processing in single visual interneurons. *Nature* 384(6608):463–66
- Krapp HG, Hengstenberg R, Egelhaaf M. 2001. Binocular contributions to optic flow processing in the fly visual system. *J. Neurophysiol.* 85(2):724–34
- Kurmangaliyev YZ, Yoo J, LoCascio SA, Zipursky SL. 2019. Modular transcriptional programs separately define axon and dendrite connectivity. *eLife* 8:e50822
- Leong JCS, Esch JJ, Poole B, Ganguli S, Clandinin TR. 2016. Direction selectivity in *Drosophila* emerges from preferred-direction enhancement and null-direction suppression. *J. Neurosci.* 36(31):8078–92
- Leonhardt A, Ammer G, Meier M, Serbe E, Bahl A, Borst A. 2016. Asymmetry of *Drosophila* ON and OFF motion detectors enhances real-world velocity estimation. *Nat Neurosci.* 19(5):706–15
- Leonhardt A, Meier M, Serbe E, Eichner H, Borst A. 2017. Neural mechanisms underlying sensitivity to reverse-phi motion in the fly. *PLOS ONE* 12(12):e0189019
- Leonte MB, Leonhardt A, Borst A, Mauss AS. 2021. Aerial course stabilization is impaired in motion-blind flies. *J. Exp. Biol.* 224(14):jeb242219
- Liu WW, Wilson RI. 2013. Glutamate is an inhibitory neurotransmitter in the *Drosophila* olfactory system. *PNAS* 110(25):10294–99
- Longden KD, Rogers EM, Nern A, Dionne H, Reiser MB. 2021. Synergy of color and motion vision for detecting approaching objects in *Drosophila*. bioRxiv 2021.11.03.467132. <https://doi.org/10.1101/2021.11.03.467132>
- Maisak MS, Haag J, Ammer G, Serbe E, Meier M, et al. 2013. A directional tuning map of *Drosophila* elementary motion detectors. *Nature* 500(7461):212–16
- Masland RH. 2012. The neuronal organization of the retina. *Neuron* 76(2):266–80
- Matulis CA, Chen J, Gonzalez-Suarez AD, Behnia R, Clark DA. 2020. Heterogeneous temporal contrast adaptation in *Drosophila* direction-selective circuits. *Curr. Biol.* 30(2):222–36
- Mauss AS, Meier M, Serbe E, Borst A. 2014. Optogenetic and pharmacologic dissection of feedforward inhibition in *Drosophila* motion vision. *J. Neurosci.* 34(6):2254–63
- Mauss AS, Pankova K, Arenz A, Nern A, Rubin GM, Borst A. 2015. Neural circuit to integrate opposing motions in the visual field. *Cell* 162(2):351–62

- Meier M, Borst A. 2019. Extreme compartmentalization in a *Drosophila* amacrine cell. *Curr. Biol.* 29(9):1545–50
- Meier M, Serbe E, Maisak MS, Haag J, Dickson BJ, Borst A. 2014. Neural circuit components of the *Drosophila* OFF motion vision pathway. *Curr. Biol.* 24(4):385–92
- Meinertzhagen IA, O’Neil SD. 1991. Synaptic organization of columnar elements in the lamina of the wild type in *Drosophila melanogaster*. *J. Comp. Neurol.* 305(2):232–63
- Mishra A, Borst A, Haag J. 2022. Voltage to calcium transformation enhances direction selectivity in *Drosophila* T4 neurons. bioRxiv 2022.07.01.498438. <https://doi.org/10.1101/2022.07.01.498438>
- O’Tousa JE, Baehr W, Martin RL, Hirsh J, Pak WL, Applebury ML. 1985. The *Drosophila ninaE* gene encodes an opsin. *Cell* 40(4):839–50
- Pankova K, Borst A. 2016. RNA-seq transcriptome analysis of direction-selective T4/T5 neurons in *Drosophila*. *PLOS ONE* 11(9):e0163986
- Pankova K, Borst A. 2017. Transgenic line for the identification of cholinergic release sites in *Drosophila melanogaster*. *J. Exp. Biol.* 220(8):1405–10
- Peek MY, Card GM. 2016. Comparative approaches to escape. *Curr. Opin. Neurobiol.* 41:167–73
- Pfeiffer BD, Jenett A, Hammonds AS, Ngo T-TB, Misra S, et al. 2008. Tools for neuroanatomy and neurogenetics in *Drosophila*. *PNAS* 105(28):9715–20
- Pinto-Teixeira F, Koo C, Rossi AM, Nericc N, Bertet C, et al. 2018. Development of concurrent retinotopic maps in the fly motion detection circuit. *Cell* 173(2):485–98
- Raji JI, Potter CJ. 2021. The number of neurons in *Drosophila* and mosquito brains. *PLOS ONE* 16(5):e0250381
- Ramón y Cajal SR, Sanchez D. 1915. *Contribución al conocimiento de los centros nerviosos de los insectos*. Madrid: Imprenta de Hijos de Nicolás Moya
- Reichardt W. 1961. Autocorrelation, a principle for the evaluation of sensory information by the central nervous system. In *Sensory Communication*, ed. WA Rosenblith, pp. 303–17. New York: MIT Press, John Wiley & Sons
- Ribeiro IMA, Drews M, Bahl A, Machacek C, Borst A, Dickson BJ. 2018. Visual projection neurons mediating directed courtship in *Drosophila*. *Cell* 174(3):607–621
- Richter FG, Fendl S, Haag J, Drews MS, Borst A. 2018. Glutamate signaling in the fly visual system. *iScience* 7:85–95
- Schiller PH, Sandell JH, Maunsell JHR. 1986. Functions of the ON and OFF channels of the visual system. *Nature* 322(6082):824–25
- Schilling T, Borst A. 2015. Local motion detectors are required for the computation of expansion flow-fields. *Biol. Open* 4(9):1105–8
- Schnell B, Raghu S, Nern A, Borst A. 2012. Columnar cells necessary for motion responses of wide-field visual interneurons in *Drosophila*. *J. Comp. Physiol. A* 198(5):389–95
- Schuetzenberger A, Borst A. 2020. Seeing natural images through the eye of a fly with remote focusing two-photon microscopy. *iScience* 23(6):101170
- Serbe E, Meier M, Leonhardt A, Borst A. 2016. Comprehensive characterization of the major presynaptic elements to the *Drosophila* OFF motion detector. *Neuron* 89(4):829–41
- Shinomiya K, Huang G, Lu Z, Parag T, Xu CS, et al. 2019. Comparisons between the ON- and OFF-edge motion pathways in the *Drosophila* brain. *eLife* 8:e40025
- Shinomiya K, Karuppudurai T, Lin TY, Lu Z, Lee CH, Meinertzhagen IA. 2014. Candidate neural substrates of off-edge motion detection in *Drosophila*. *Curr. Biol.* 24(10):1062–70
- Shinomiya K, Nern A, Meinertzhagen IA, Plaza SM, Reiser MB. 2022. Neuronal circuits integrating visual motion information in *Drosophila melanogaster*. *Curr. Biol.* 32(16):3529–44.e2
- Silies M, Gohl DM, Fisher YE, Freifeld L, Clark DA, Clandinin TR. 2013. Modular use of peripheral input channels tunes motion-detecting circuitry. *Neuron* 79(1):111–27
- Single S, Borst A. 1998. Dendritic integration and its role in computing image velocity. *Science* 281(5384):1848–50
- Single S, Haag J, Borst A. 1997. Dendritic computation of direction selectivity and gain control in visual interneurons. *J. Neurosci.* 17(16):6023–30
- Stavenga DG. 2003a. Angular and spectral sensitivity of fly photoreceptors. I. Integrated facet lens and rhabdomere optics. *J. Comp. Physiol. A* 189(1):1–17

- Stavenga DG. 2003b. Angular and spectral sensitivity of fly photoreceptors. II. Dependence on facet lens F-number and rhabdomere type in *Drosophila*. *J. Comp. Physiol. A* 189(3):189–202
- Strausfeld NJ. 1971. The organization of the insect visual system (light microscopy). *Z. Zellforsch.* 121:377–441
- Strother JA, Nern A, Reiser MB. 2014. Direct observation of ON and OFF pathways in the *Drosophila* visual system. *Curr. Biol.* 24(9):976–83
- Strother JA, Wu ST, Wong AM, Nern A, Rogers EM, et al. 2017. The emergence of directional selectivity in the visual motion pathway of *Drosophila*. *Neuron* 94(1):168–82
- Takemura S, Bharioke A, Lu Z, Nern A, Vitaladevuni S, et al. 2013. A visual motion detection circuit suggested by *Drosophila* connectomics. *Nature* 500(7461):175–81
- Takemura SY, Lu Z, Meinertzhagen IA. 2008. Synaptic circuits of the *Drosophila* optic lobe: the input terminals to the medulla. *J. Comp. Neurol.* 509(5):493–513
- Takemura SY, Karuppudurai T, Ting CY, Lu Z, Lee CH, Meinertzhagen IA. 2011. Cholinergic circuits integrate neighboring visual signals in a *Drosophila* motion detection pathway. *Curr. Biol.* 21(24):2077–84
- Takemura SY, Nern A, Chklovskii DB, Scheffer LK, Rubin GM, Meinertzhagen IA. 2017. The comprehensive connectome of a neural substrate for ‘ON’ motion detection in *Drosophila*. *eLife* 6:e24394
- Tuthill JC, Chiappe ME, Reiser MB. 2011. Neural correlates of illusory motion perception in *Drosophila*. *PNAS* 108(23):9685–90
- Tuthill JC, Nern A, Holtz SL, Rubin GM, Reiser MB. 2013. Contributions of the 12 neuron classes in the fly lamina to motion vision. *Neuron* 79(1):128–40
- Wardill TJ, List O, Li X, Dongre S, McCulloch M, et al. 2012. Multiple spectral inputs improve motion discrimination in the *Drosophila* visual system. *Science* 336(6083):925–31
- Wernet MF, Mazzoni EO, Çelik A, Duncan DM, Duncan I, Desplan C. 2006. Stochastic spineless expression creates the retinal mosaic for colour vision. *Nature* 440(7081):174–80
- Wienecke CFR, Leong JCS, Clandinin TR. 2018. Linear summation underlies direction selectivity in *Drosophila*. *Neuron* 99(4):680–88
- Yamaguchi S, Wolf R, Desplan C, Heisenberg M. 2008. Motion vision is independent of color in *Drosophila*. *PNAS* 105(12):4910–15
- Yang HH, St-Pierre F, Sun X, Ding X, Lin MZ, Clandinin TR. 2016. Subcellular imaging of voltage and calcium signals reveals neural processing in vivo. *Cell* 166(1):245–57
- Zavatone-Veth JA, Badwan BA, Clark DA. 2020. A minimal synaptic model for direction selective neurons in *Drosophila*. *J. Vis.* 20(2):2



Contents

Therapeutic Potential of PTBP1 Inhibition, If Any, Is Not Attributed to Glia-to-Neuron Conversion <i>Lei-Lei Wang and Chun-Li Zhang</i>	1
How Flies See Motion <i>Alexander Borst and Lukas N. Groschner</i>	17
Meningeal Mechanisms and the Migraine Connection <i>Dan Levy and Michael A. Moskowitz</i>	39
Cholesterol Metabolism in Aging and Age-Related Disorders <i>Gesine Saher</i>	59
Spinal Interneurons: Diversity and Connectivity in Motor Control <i>Mohini Sengupta and Martha W. Bagnall</i>	79
Astrocyte Endfeet in Brain Function and Pathology: Open Questions <i>Blanca Díaz-Castro, Stefanie Robel, and Anusha Mishra</i>	101
Circadian Rhythms and Astrocytes: The Good, the Bad, and the Ugly <i>Michael H. Hastings, Marco Brancaccio, Maria F. Gonzalez-Apone, and Erik D. Herzog</i>	123
Therapeutic Potential of PTB Inhibition Through Converting Glial Cells to Neurons in the Brain <i>Xiang-Dong Fu and William C. Mobley</i>	145
How Instructions, Learning, and Expectations Shape Pain and Neurobiological Responses <i>Lauren Y. Atlas</i>	167
Cognition from the Body-Brain Partnership: Exaptation of Memory <i>György Buzsáki and David Tingley</i>	191
Neural Circuits for Emotion <i>Meryl Malezieux, Alexandra S. Klein, and Nadine Gogolla</i>	211
The Computational and Neural Bases of Context-Dependent Learning <i>James B. Heald, Daniel M. Wolpert, and Máté Lengyel</i>	233

Integration of Feedforward and Feedback Information Streams in the Modular Architecture of Mouse Visual Cortex <i>Andreas Burkhalter, Rinaldo D. D’Souza, Weiqing Ji, and Andrew M. Meier</i>	259
How Do You Build a Cognitive Map? The Development of Circuits and Computations for the Representation of Space in the Brain <i>Flavio Donato, Anja Xu Schwartzlose, and Renan Augusto Viana Mendes</i>	281
Cortical Integration of Vestibular and Visual Cues for Navigation, Visual Processing, and Perception <i>Sepiedeh Keshavarzi, Mateo Velez-Fort, and Troy W. Margrie</i>	301
Neural Control of Sexually Dimorphic Social Behavior: Connecting Development to Adulthood <i>Margaret M. McCarthy</i>	321
Deep Brain Stimulation for Obsessive-Compulsive Disorder and Depression <i>Sameer A. Sheth and Helen S. Mayberg</i>	341
Striosomes and Matrisomes: Scaffolds for Dynamic Coupling of Volition and Action <i>Ann M. Graybiel and Ayano Matsushima</i>	359
Specialized Networks for Social Cognition in the Primate Brain <i>Ben Deen, Caspar M. Schwiedrzik, Julia Sliwa, and Winrich A. Freiwald</i>	381
Neural Networks for Navigation: From Connections to Computations <i>Rachel I. Wilson</i>	403

Indexes

Cumulative Index of Contributing Authors, Volumes 37–46	425
---	-----

Errata

An online log of corrections to *Annual Review of Neuroscience* articles may be found at
<http://www.annualreviews.org/errata/neuro>